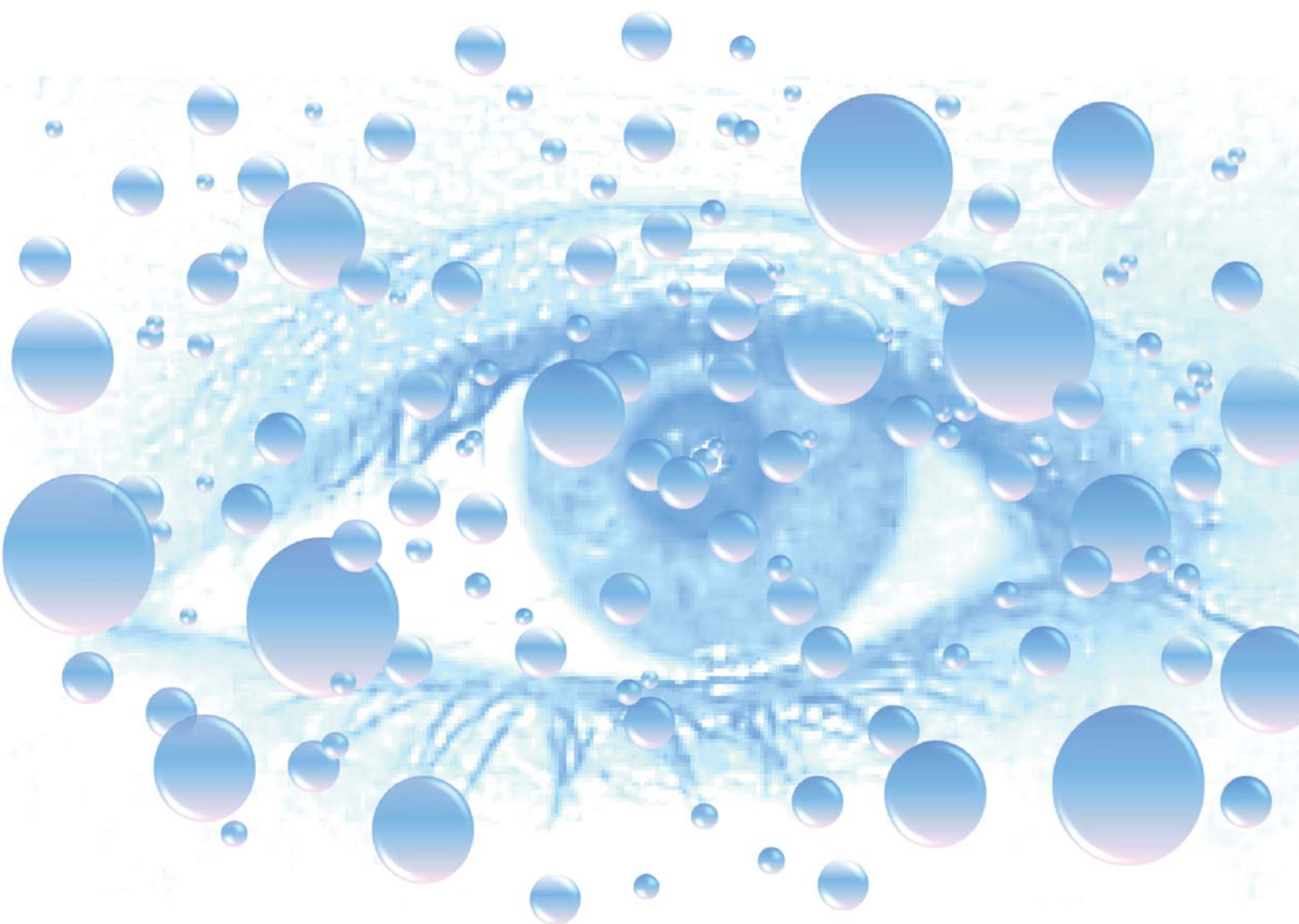


# Soft Matter

[www.rsc.org/softmatter](http://www.rsc.org/softmatter)

Volume 7 | Number 17 | 7 September 2011 | Pages 7569–7876



Themed issue: Dynamics and Rheology of Complex Fluid–Fluid Interfaces

ISSN 1744-683X

RSC Publishing

**PAPER**  
Jennifer J. McManus and  
Alfred J. Crosby *et al.*  
Cavitation rheology of the eye lens



International Year of  
**CHEMISTRY**  
2011



1744-683X(2011)7:17;1-G

Cite this: *Soft Matter*, 2011, **7**, 7827

www.rsc.org/softmatter

PAPER

## Cavitation rheology of the eye lens†

Jun Cui,<sup>a</sup> Cheol Hee Lee,<sup>a</sup> Aline Delbos,<sup>a</sup> Jennifer J. McManus<sup>\*b</sup> and Alfred J. Crosby<sup>\*a</sup>

Received 24th February 2011, Accepted 10th May 2011

DOI: 10.1039/c1sm05340j

The anisotropic mechanical properties of bovine eye lenses were measured using cavitation rheology over a range of length scales. The technique involves inducing a cavity at the tip of a syringe needle in different regions of the lens. Effective Young's moduli of the nucleus and cortex of the lens were determined, as approximately 11.8 and 0.8 kPa, respectively, on macroscopic length scales. We also measured the mechanical properties of the lens on the length scale of a single cell, suggesting that the stiffness significantly decreased from that in the bulk measurements for both the nucleus and cortex. In addition, during the growth of the cavity anisotropic propagation in the cortex was observed, while in the nucleus, the propagation was isotropic. We further explored the elasticity of the cavity deformation, showing both elastic and inelastic deformation occurred in the nucleus with equal contributions while deformation in the cortex was elastic and reversible.

### Introduction

Understanding the mechanical properties of the eye lens is important in understanding eye diseases. For example, presbyopia, a condition commonly observed in elderly people, is caused by a loss of elasticity in the eyes, which is reflected by a significant increase in stiffness of the eye lenses with increasing age.<sup>1</sup> The stiffness of the eye lenses has been characterized by a variety of techniques, such as tensile test,<sup>2</sup> spinning measurements,<sup>3</sup> dynamic analysis<sup>4–6</sup> and contact mechanics.<sup>7</sup> However, disadvantages still exist with these techniques. Most of them are applied to the capsule of the lens, where the composition and elasticity are different from those of the cells inside the bulk of the lens, thus making the measured stiffness complicated to interpret. Furthermore, existing testing methods lack the ability to measure microscopic heterogeneities, which significantly contribute to the function of the eye lens.

The eye lens, like other biological tissues, has a complex structure. It consists of three regions: the lens capsule, the lens epithelium and the lens fiber cells.<sup>8</sup> The fiber cells, which constitute the majority of the lens, are differentiated from the epithelium and displaced toward the center, resulting in a layered structure. By periods of growth, the fiber cells are further divided into two distinct regions, the nuclear core and the cortex.<sup>9</sup> The nuclear cells are round with an area of approximately 80  $\mu\text{m}^2$ ,

while the cortical cell fibers are irregularly hexagonal with an average cross-sectional area of approximately 24  $\mu\text{m}^2$ .<sup>10</sup> The lens fibers are composed mainly of proteins at high concentration, which give the lens its high refractive index. Short-range liquid-like order of the proteins inside the eye lens account for its transparency.<sup>11</sup> These proteins, mostly  $\alpha$ -,  $\beta$ - and  $\gamma$ -crystallins, are the major protein constituents of the eye lens, and can represent up to 35% of the mass of the tissue. The crystallin proteins are distributed in different amounts throughout the lens.  $\gamma$ -Crystallins, predominately synthesized prenatally, are concentrated in the nucleus, while  $\beta$ -crystallins distribute as the mirror image of the  $\gamma$ -crystallins, mostly concentrated in the cortex.  $\alpha$ -Crystallins are distributed equally throughout the whole lens.<sup>12</sup> Cataract disease, which involves the condensation of the crystallin proteins within the eye lens resulting in lens opacity, is due to the formation of high molecular weight aggregates of crystallin proteins. These changes result in greater heterogeneity within the lens, particularly with increasing age. It has been shown that the backscattering of light from these aggregates increases exponentially with age.<sup>13</sup> The lens fibers are unusual in that for mature lenses, the nucleus, endoplasmic reticulum and mitochondria are absent, contributing to the overall transparency of the lens. The lens fibers also have an extensive cytoskeleton helping to maintain consistent packing of the cell structure. These differences in protein compositions, as well as in the geometry and arrangement of the cells, lead to the anisotropic mechanical properties of the lens on macroscopic length scales.

To better understand and quantify the anisotropic properties of the lens, recently, Heys *et al.*<sup>14</sup> investigated the mechanics of the nuclear and cortical regions in human lenses as a function of age using a dynamic mechanical analyzer. They found that the stiffness across the equatorial plane was different with increasing

<sup>a</sup>Department of Polymer Science and Engineering, University of Massachusetts, 120 Governors Dr Amherst, MA, 01003, USA. E-mail: crosby@mail.pse.umass.edu; Fax: +1 413 545 0082; Tel: +1 413 577 1313

<sup>b</sup>Department of Chemistry, National University of Ireland Maynooth, Maynooth, Co. Kildare, Ireland. E-mail: jennifer.mcmanus@nuim.ie; Fax: +353 708 3815; Tel: +353 1 708 6926

† Electronic supplementary information (ESI) available. See DOI: 10.1039/c1sm05340j

age, suggesting the increase in the stiffness of the nucleus was more pronounced than that of the cortex. Those results were consistent with the age dependent alterations in accommodation of the lens, which could be a major contributing factor to presbyopia. However, the measurements required sectioning of the lenses in addition to a freezing process, which lead to an inevitable overestimation.<sup>5</sup>

Therefore, a technique that is capable of measuring the mechanical properties across a range of length scales of tissues *in vivo* is a necessity to better understand the anisotropic mechanical properties, as well as the microscopic heterogeneities.<sup>15</sup>

In this paper, we report and discuss mechanical measurements on the nucleus and cortex in the bovine lens using cavitation rheology, a recently developed technique with a distinct advantage for measuring elasticity across a range of length scales, from sub-micron to millimeter.<sup>15,16</sup> In these measurements, a syringe needle was inserted into the sample, inducing an elastic instability by slow pressurization with air or liquid as the medium. The elastic deformation at the point of instability, or the cavity, grows isotropically in homogeneous materials, such as a polyacrylamide gel in Fig. 1. Previous investigations<sup>16,17</sup> have shown that Young's modulus measured by cavitation rheology is consistent with that measured by contact mechanics and parallel plate shear rheometry with the assumption that the stress is isotropically distributed when the instability occurs.

The critical pressure ( $P_c$ ) to induce the instability is related to the mechanical properties (*e.g.* Young's modulus,  $E$ ) of the sample, as well as the surface tension ( $\gamma$ ) between the sample and the medium, as shown here:<sup>16,17</sup>

$$P_c = 5E/6 + 2\gamma/r \quad (1)$$

where  $r$  is the inner radius of the needle. This equation is based on the assumption that the stress is isotropically distributed in the materials. According to the equation, the critical pressure plotted for various needle radii provides information on the mechanical properties and the surface tension, which are independent of the orientation of the surroundings. The cavitation process is elastic and reversible, reflected in the assumptions leading to eqn (1), but it is also known that irreversible deformation or fracture may occur prior to cavitation, depending upon the material and needle radius.<sup>17</sup> In the case of fracture,  $P_c$  scales with  $r^{1/2}$ .<sup>17</sup> To induce cavitation, either air or liquid can be used. In previous investigations, air shows success in measuring the elastic and surface properties on both synthetic hydrogels<sup>16,17</sup> and biological tissues.<sup>18</sup> Liquid, such as water, can also be used to induce the

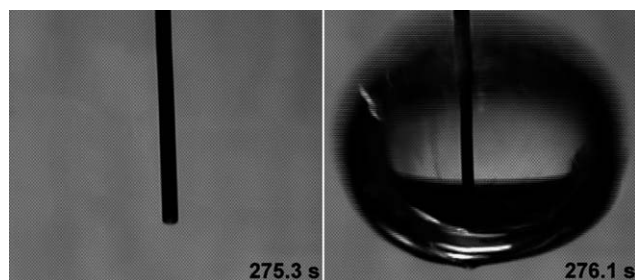


**Fig. 1** Micrographs of initiation and propagation of a cavity in 2.7% polyacrylamide gel. The inner radius of the syringe needle is 80  $\mu\text{m}$ .

elastic instability with negligible interfacial tension with the surrounding material, thus providing a useful tool to study complex materials, especially at small length scales where the surface tension may dominate the magnitude of  $P_c$  and diminish the sensitivity to mechanical property contributions.<sup>19</sup> Here, we conduct cavitation rheology on bovine eye lenses with both air and water over a range of length scales to quantify the elastic behaviors of different spatial regions in the lens, particularly in the nuclear and cortical regions. These measurements demonstrate the capability of cavitation rheology in measuring the complex heterogeneous properties in biological tissues, and, at the same time, they provide understanding of the impact of well-known anisotropic structures on cavitation rheology measurements.

## Experimental

### Materials

Bovine eyes were provided by Research 87 (Boylston, Massachusetts) and used within 48 h post-mortem. The calves were either Jersey or Holstein males between 2 and 10 days old and were certified disease free. The eyes were stored at 8  $^{\circ}\text{C}$  and allowed to warm to room temperature before experiments. The lens was extracted from the eye by incising between the cornea and the sclera.

### Instruments

The cavitation rheology instrument used to perform the measurements is shown in Fig. 2a and has been discussed previously.<sup>16</sup> In short, the instrument consists of a syringe pump (New Era Syringe Pump), pressure sensor (Omega Engineering), syringe needle (Fisher Scientific), translation stage (Newport), microscope (Edmund Optics), camera (Edmund Optics) and personal computer to record the pressure and images during the measurements. The lens was placed on the translation stage, which was used to adjust the position of the needle to different regions within the lens. The center of the lens was determined by

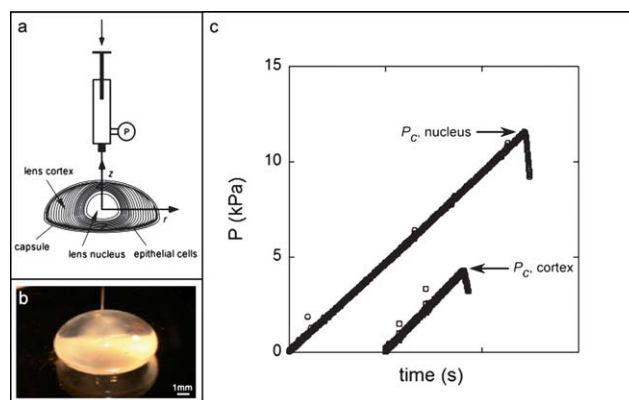


**Fig. 2** (a) Schematic illustration of the cavitation rheology experiment on the eye lens. (b) Micrograph of a bovine lens during measurements. Needle is shown entering the lens at the top. (c) A representative plot of pressure as a function of time during measurements for both nucleus and cortex with air using a same syringe needle with inner radius of 55  $\mu\text{m}$ . The data for the cortex have been shifted arbitrarily along the time axis for clarity purposes.

the apex of the lens curvature from multiple perspectives to establish the position of  $r = 0$ ,  $z = h$ . Measurements on the nuclear region begin by positioning the needle at  $r = 0$ ,  $z = h$  and then inserting the needle to a depth of  $h-5 \text{ mm} < z < h-3 \text{ mm}$ . For the measurements of the cortex, the position of the needle was adjusted to  $r > 3 \text{ mm}$  (although this varied depending on the size of the lens to ensure needle placement was clearly in the cortex) and a depth of  $h-5 \text{ mm} < z < h-3 \text{ mm}$ . After establishing the position, the compression of the media within the syringe and needle was initiated *via* the syringe pump. For all measurements, the rate of compression was  $400 \mu\text{L min}^{-1}$  for air and  $50 \mu\text{L min}^{-1}$  for water. The pressure was recorded at a frequency of 10 Hz.

## Results and discussion

Fig. 2c demonstrates the pressure change as a function of time for both the nucleus and cortex of the lens in the cavitation rheology measurements. A cavity formed and propagated spontaneously when critical pressure ( $P_c$ ) was reached, reflected by a significant decrease of pressure after the critical point, and is consistent with previous cavitation rheology measurements on both synthetic and biological materials. The deformation occurred in seconds, which is significantly shorter than the relaxation time of the lens, approximately 3 minutes, as measured by Kikkawa and Sato<sup>20</sup> using a mechano-electric transducer. In addition, previous visco-elastic measurements also suggested that the storage modulus was independent of frequency, ranging from 0.01 to 25 Hz, and the value for the loss tangent was 0.3–0.4 in the same frequency range.<sup>4</sup> Furthermore, the extension ratio at the onset of the cavity was estimated by taking the ratio of the cavity surface area to the cross-sectional area of the inner syringe radius,  $\lambda = (A_0/A_{0c})^{1/2}$ . For both the nucleus and cortex,  $\lambda$  varied from 1.1 to 1.3.

The critical pressure was measured as a function of different syringe needle sizes, ranging from  $55 \mu\text{m}$  to  $300 \mu\text{m}$ . Assuming the stress is isotropically distributed in the materials, the effective Young's moduli are obtained by plotting  $P_c$  as a function of inner radius of the needles according to eqn (1) (Fig. 3).

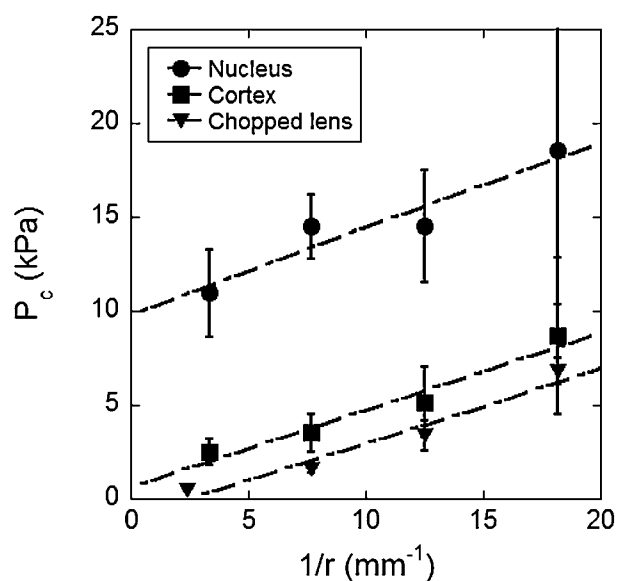


Fig. 3 Changes in critical pressure as a function of needle radius for the bovine lens nucleus, cortex and chopped lens with air.

Measured values are approximately 0.8 and 11.8 kPa for cortex and nucleus, respectively, consistent with the average Young's modulus characterized by spinning methods for human eyes, ranging from 0.4 to 3.6 kPa.<sup>3</sup> The increase in stiffness from cortex to nucleus has also been observed by dynamic mechanical analysis, which suggested that Young's modulus was 0.8 kPa in the cortex and 1.4 kPa in the nucleus for human lenses from 40 year old people.<sup>14</sup> Although mechanical characterization of bovine lenses has not been reported in the literature, bovine eyes resemble human tissues in their composition and function.<sup>12</sup> The similarity further confirmed that the stiffness values measured in bovine eyes are consistent with those reported for human eyes. Although the values measured by the cavitation rheology technique are consistent with those by the macroscopic techniques as we compare the effective  $E$ , a more detailed analysis will be required to quantify the elastic constants associated with the lens anisotropy on different length scales, which will be investigated in the future.

Surface tension values were also measured according to eqn (1). The measured values are  $0.21$  and  $0.23 \text{ N m}^{-1}$  for the cortex and nucleus, respectively. The values are similar in the two regions, suggesting similar chemical environments in bovine eyes. Since surface tension is strongly dependent upon composition and weakly on size of molecular units,<sup>21</sup> we confirmed the surface tension values by performing measurements on a bovine lens sample that was chopped and mixed in order to disrupt the elasticity-producing structures. In the absence of elasticity, the critical pressure  $P_c \approx 2\gamma/r$ , where  $\gamma$  is the surface tension between the cavitation medium and the specimen. As shown in Fig. 3, the surface tension value acquired from the fitting is consistent with the cortex and nucleus measurements, approximately  $0.2 \text{ N m}^{-1}$  for the chopped lens.

Measurements were also performed by inducing cavitation with water (Fig. 4), which enables investigation on microscopic scales by decreasing the contribution of surface tension. Across the length scales of  $55 \mu\text{m}$  to  $300 \mu\text{m}$ , the elastic behavior of the nucleus and the cortex are consistent with those measured with air, in that the cortex possesses an effective Young's modulus of 0.7 kPa, softer than the nucleus with a modulus of 9.1 kPa. In comparison to the surface tension measured with air, the surface tension between the lens and water is significantly decreased. For the nucleus and cortex,  $\gamma \approx 0.1$  and  $0.09 \text{ N m}^{-2}$ , respectively. For measurements with  $r = 5 \mu\text{m}$ , comparable with the sizes of lens cells,<sup>10</sup> the critical pressure was measured to be significantly less than  $P_c$  estimated according to eqn (1). Using eqn (1) and surface tension values determined for larger needle radii,  $P_c$  should be equal to 48 kPa for the nucleus and 35 kPa for the cortex at  $r = 5 \mu\text{m}$ . This deviation suggests that the elasticity in the scale of single cells is different from that in macroscopic measurements. Furthermore, a large statistical deviation in the  $P_c$  value is observed, which may reflect heterogeneities of lenses from various specimens at microscopic length scales.

Cavitation rheology not only can be used to quantitatively measure the stiffness of the nucleus and cortex upon the onset of the cavity but also can provide information on the anisotropic properties of the lens. The propagation or growth of the cavity is related to the surrounding materials. As discussed above, cavitation in an elastic homogeneous material is a spherical void. As shown in Fig. 5, this spherical growth behavior is observed in the

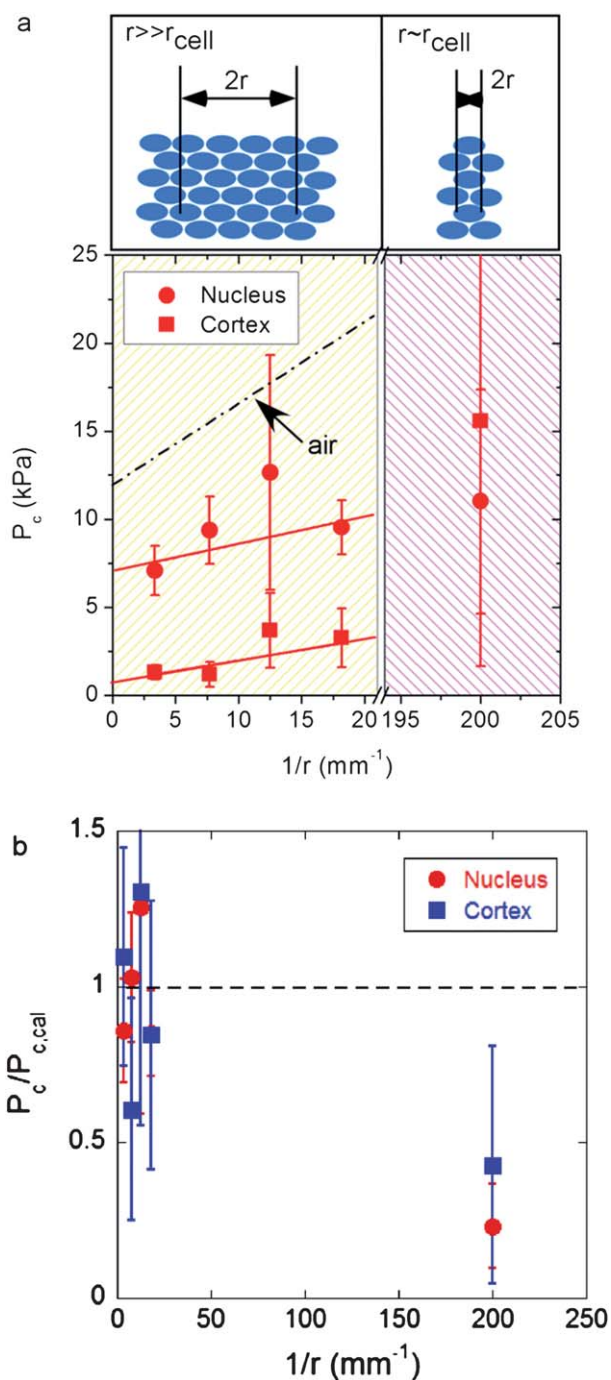


**Fig. 4** (a) Changes in critical pressure as a function of needle radius across a range of length scales for the bovine nucleus and cortex with water. The dashed line shows the trend of critical pressure as a function of needle radius with air and has been shifted arbitrarily along the  $P_c$  axis for clarity purposes. (b) The ratio of the measured  $P_c$  and  $P_{c,\text{cal}}$  calculated by the fitting curve according to eqn (1) as a function of needle radius. The dashed line indicates that the measured  $P_c$  is equal to the calculated  $P_c$ .

nucleus. The isotropic properties were also observed by Itoi *et al.* in their dynamic rheology measurements on nucleus cubes, showing the same mechanical properties, regardless of the direction of the cut, relative to the regular arrangement of the lens fibers.<sup>4</sup> In contrast, the onset of cavitation in the cortex leads to anisotropic growth of a void, where the void grows

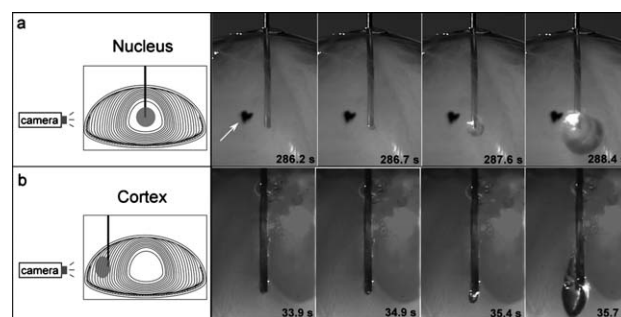


**Fig. 5** Micrographs of initiation and propagation of cavities in the regions of nucleus (top) and cortex (bottom). The inner radius of the syringe needle is  $55 \mu\text{m}$ . The black defect shown in the nucleus images is a piece of zonule left during extraction.

preferentially toward the periphery of the lens. During cavity propagation, the change in pressure, reflected by the slope change after the critical point is slightly different for nucleus and cortex (ESI Fig. 1a†). To account for the initial volume compressed in the system by normalizing the slope by the critical pressure, the same normalized slope is observed for nucleus and cortex, as shown in ESI Fig. 1b†, suggesting that the isotropic and anisotropic deformation in the lens is proceeding at the same volumetric rate. The observed growth of the cavity in the cortex toward the periphery of the lens is consistent with the cavity growth in a material that has a decreasing stiffness gradient in the radial direction. In cavitation rheology measurements described here, the volume of the syringe is decreased while the number of air molecules is fixed. This results in an increase in pressure exerted on the air-specimen interface at the tip of the syringe needle until  $P_c$  is reached. At  $P_c$ , for materials where elasticity dominates surface energy, or the ratio of  $\gamma/Er$  is less than unity, the cavity will grow in directions that minimize the elastic strain energy of the system. For anisotropic materials, the maximum decrease in elastic strain energy will bias growth toward the softest material directions, which in the lens is in the outward radial direction.

The previous discussion of observed results assumed that the instability deformation was due to cavitation, an elastic reversible process, in contrast to fracture. In addition to the linear scaling observed between  $P_c$  and  $1/r$  at large length scales, we have also quantified the reversibility of the induced deformation. The measurements were performed by multiple pressurization and depressurization cycles with air and the pressure was recorded as a function of time in Fig. 6. In these measurements, air was compressed at a constant rate,  $300 \mu\text{L min}^{-1}$ , until cavitation occurred, and the pressure was released by dissipating the compressed air into a formed cavity. After cavitation, the air in the cavity was retracted by depressurizing the system at the same rate until the pressure was constant and approximately zero. For the cortex, cavitation was observed to occur at similar critical pressure values for sequential cycles, which suggests the primary deformation is reversible and no permanent damage occurs within the tissue. In the nucleus,  $P_c$  in the second cycle is reduced as compared to the first cycle, and  $P_c$  for subsequent events are similar to the second event. This decrease in  $P_c$  indicates that irreversible deformation occurs during the first initiation events; however, the nature of the deformation is different

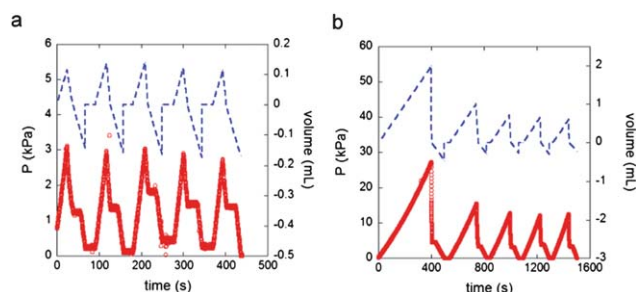


**Fig. 6** Pressure changes as a function of time for the cortex (a) and nucleus (b) by running multiple pressurization and depressurization cycles as red dots, with volume change in the system as blue dashed line.

from fracture observed in previous measurements on synthetic polyacrylamide gels where fracture is related to permanent chain incision.<sup>17</sup> For the nucleus, a decreased but constant critical pressure exists on the second and subsequent cycles, suggesting the initial deformation consists of elastic and inelastic contributions of similar magnitude. After the initial deformation, the elastic contribution still provides a mechanism for an observed elastic instability event.

## Conclusions

In this paper, we have demonstrated the use of cavitation rheology in determining the elastic properties of two different regions in the bovine lens and have used the known anisotropic structures of the lens to understand the impact of anisotropic properties on cavitation rheology measurements. Our results have shown that the effective Young's modulus of the nucleus is higher than that of the cortex on the length scales that are greater than the length scale of a single cell, while a similar stiffness is observed for the two regions on the length scales of a single cell. Furthermore, our research also suggests that isotropic propagation of cavity occurs in the nucleus with elastic and inelastic deformation equally contributed, while elastic anisotropic deformation in the cortex is observed.

## Acknowledgements

The authors would like to acknowledge NSF PIRE (NSF-0730243) and the Army Research Laboratory through the Center for University of Massachusetts Industry Research on Polymers Cluster M for funding. JMcM would like to acknowledge Science Foundation Ireland Stokes Lectureship and the Royal Irish Academy Mobility Grant for funding.

## Notes and references

- 1 D. A. Atchison, *Ophthalmic and Physiological Optics*, 1995, **15**, 255–272.
- 2 G. W. van Alphen and W. P. Graebel, *Vision Research*, 1991, **31**, 1417–1438.
- 3 R. F. Fisher, *Exp. Eye Res.*, 1971, **11**, 143–180.
- 4 M. Itoi, N. Ito and H. Kaneko, *Exp. Eye Res.*, 1965, **4**, 168–173.
- 5 H. A. Weeber, G. Eckert, F. Soergel, C. H. Meyer, W. Pechhold and R. G. L. van der Heijde, *Exp. Eye Res.*, 2005, **80**, 425–434.
- 6 G. Czygan and C. Hartung, *Med. Eng. Phys.*, 1996, **18**, 345–349.
- 7 N. M. Ziebarth, E. P. Wojcikiewicz, F. Manns, V. T. Moy and J. M. Parel, *Mol. Vision*, 2007, **13**, 504–510.
- 8 H. Bloemendal, *Science*, 1977, **197**, 127–138.
- 9 R. C. Augusteyn, *Exp. Eye Res.*, 2010, **90**, 643–654.
- 10 V. L. Taylor, K. J. AlGhoul, C. W. Lane, V. A. Davis, J. R. Kuszak and M. J. Costello, *Invest. Ophthalmol. Visual Sci.*, 1996, **37**, 1396–1410.
- 11 G. B. Benedek, *Appl. Opt.*, 1971, **10**, 459–473.
- 12 R. C. Augusteyn and A. Stevens, *Prog. Polym. Sci.*, 1998, **23**, 375–413.
- 13 G. M. Thurston, D. L. Hayden, P. Burrows, J. I. Clark, V. G. Taret, J. Kandel, M. Courogen, J. A. Peetermans, M. S. Bowen, D. Miller, K. M. Sullivan, R. Storb, H. Stern and G. B. Benedek, *Curr. Eye Res.*, 1997, **16**, 197–207.
- 14 K. R. Heys, S. L. Cram and R. J. W. Truscott, *Mol. Vision*, 2004, **10**, 956–963.
- 15 A. J. Crosby and J. J. McManus, *Phys. Today*, 2011, **67**, 62–63.
- 16 J. A. Zimmerlin, N. Sanabria-DeLong, G. N. Tew and A. J. Crosby, *Soft Matter*, 2007, **3**, 763–767.
- 17 S. Kundu and A. J. Crosby, *Soft Matter*, 2009, **5**, 3963–3968.
- 18 J. A. Zimmerlin, J. J. McManus and A. J. Crosby, *Soft Matter*, 2010, **6**, 3632–3635.
- 19 J. A. Zimmerlin and A. J. Crosby, *J. Polym. Sci., Part B: Polym. Phys.*, 2010, **48**, 1423–1427.
- 20 Y. Kikkawa and T. Sato, *Exp. Eye Res.*, 1963, **2**, 210–215.
- 21 R. A. L. Jones and R. W. Richards, *Polymers at Surfaces and Interfaces*, Cambridge University Press, Cambridge; New York, 1999.